Carbohydrate Polymers 80 (2010) 655–664

Contents lists available at ScienceDirect

Carbohydrate Polymers

journal homepage: www.elsevier.com/locate/carbpol

Chitosan, sisal cellulose, and biocomposite chitosan/sisal cellulose films prepared from thiourea/NaOH aqueous solution

E.V.R. Almeida [a,b], E. Frollini [b,*], A. Castellan [a], V. Coma [a,*]

[a] UMR 5103 Unité des Sciences du Bois et des Biopolymères – US2B, Université Bordeaux 1, INRA, CNRS, 351 cours de la Libération, 33405 Talence, France
[b] Instituto de Química de São Carlos, Universidade de São Paulo, C P 780, 13560 970 São Carlos, SP, Brazil

ARTICLE INFO

Article history:
Received 26 May 2009
Received in revised form 9 October 2009
Accepted 15 October 2009
Available online 23 October 2009

Keywords:
Chitosan–cellulose films
Biocomposite
NaOH/thiourea aqueous solutions

ABSTRACT

Environmentally friendly biocomposites were successfully prepared by dissolving chitosan and cellulose in a NaOH/thiourea solvent with subsequent heating and film casting. Under the considered conditions, NaOH/thiourea led to chain depolymerization of both biopolymers without a dramatic loss of film forming capacities. Compatibility of both biopolymers in the biocomposite was firstly assessed through scanning electron microscopy, revealing an intermediate organization between cellulose fiber network and smoothness of pure chitosan. DSC analyses led to exothermic peaks close to 285 and 315 °C for the biocomposite, compared to the exothermic peaks of chitosan (275 °C) and cellulose (265 and 305 °C), suggesting interactions between chitosan and cellulose. Contact angle analyses pointed out the deformation that can occur at the surface due to the high affinity of these materials with water. T_2 NMR relaxometry behavior of biocomposites appeared to be dominated by chitosan. Other properties of films, as crystallinity, water sorption isotherms, among others, are also discussed.

1. Introduction

Advanced technology in the field of petrochemical-based polymers has brought many benefits to mankind. It is becoming more evident that the ecosystem is considerably disturbed and damaged as a result of the non-degradable plastic materials for disposable items (Lu, Weng, & Cao, 2006). So there is an urgent need to develop materials from renewable resources, which would be of great importance to the materials domain, not only as a solution to growing environmental threat but also as a solution to the uncertainty of petroleum supply. Among the many kinds of candidates of biodegradable polymer, cellulose is one of the most promising materials for biodegradable plastics, because it is a versatile biopolymer with immense potential and low price for use in the non-food industries.

Recently, in addition to liquid ionic solvents (Cao et al., 2009; Feng & Che, 2008), research efforts have been made on the elaboration of cellulose film forming solution using cheap and non-polluting direct solvent such as alkaline ones. Zhang, Mao, Zhou, and Cai (2005) studied the dissolution of cellulose by NaOH/urea aqueous solvent and the ^{13}C NMR spectra suggested the complete dissolution of the biopolymer and also that intra-molecular hydrogen bonds have been destroyed in this solution. These authors mentioned that NaOH creates a significant ion-pair interaction favoring new intermolecular interaction between urea and cellulose. The chemical shifts obtained were the same as those obtained from LiCl-DMAc, a non-derivatizing solvent of cellulose (Ramos, Assaf, El Seoud, & Frollini, 2005). Cellulose films with good properties were obtained after a coagulation procedure with an optimal coagulant H_2SO_4 (5% wt.)/Na_2SO_4 (5% wt.) aqueous solution. Moreover Zhang, Ruan, and Gao (2002) specified that NaOH aqueous solution containing thiourea, dissolved cellulose more easily than NaOH/urea aqueous solutions. NaOH/thiourea appeared also as a direct solvent of the cellulose rather than a derivative aqueous solution system.

However, compared to common thermoplastics, biosourced products based on cellulose, still reveal unfortunately some disadvantages, such as low mechanical properties and moisture sensitivity. One of the effective strategies, allowing to maintain the biodegradability, is to elaborate biocomposites by association of cellulose with other biopolymers exhibiting film forming properties and derived from renewable resources.

Chitosan is a linear high molecular weight aminopolysaccharide and a major component of insects and crustaceans shells. Obviously, it is biodegradable, environmentally clean and bioactive (Desbrières, 2002; Kumar, Bristow, Smith, & Payne, 2000; Muzzarelli & Muzzarelli, 2005). Owing to their biodegradability and bioactivity, homopolymers and copolymers of chitosan have been widely used in packaging material applications (Arvanitoyannis, Nakayama, & Aiba, 1998; Coma, 2008; Coma et al., 2002; Fimbeau, Grelier, Copinet, & Coma, 2005; Möller, Grelier, Pardon, & Coma,

* Corresponding authors. Tel.: +33 05 40 00 29 13 (V. Coma).
E-mail addresses: V.coma@us2b.u-bordeaux1.fr, v.coma@lcsv.u-bordeaux1.fr (V. Coma).

0144-8617/$ - see front matter © 2010 Published by Elsevier Ltd.
doi:10.1016/j.carbpol.2009.10.039

2004). In parallel, there is an increased interest in preparing chitosan/polymer blends for different applications, such as biomaterial applications (Arvanitoyannis, Kolokuris, Nakayama, Yamamoto, & Aiba, 1997; Luo, Yin, Khutoryanskaya, & Khutoryanskiy, 2008; Molinaro, Leroux, Damas, & Adam, 2002; Park et al., 2001; Siddaramaiah, Divya, Mhemavathi, & Manjula, 2006; Zhao, Mitomo, & Yosh, 2008). The presence of amino groups makes chitosan soluble in dilute aqueous solutions of common acids.

Because of its properties such as bioactivity, high mechanical strength and moisture transfer generally lower than pure cellulose films, a combination of chitosan with cellulose as blends could produce biocomposites with novel properties (Hasegawa, Isogai, Kuga, & Onabe, 1994; Hasegawa, Isogai, Onabe, & Usuda, 1992; Hasegawa, Isogai, Onabe, Usuda, & Atalla, 1992; Isogai & Atalla, 1992; Li, Zhuang, Liu, Guan, & Yao, 2002; Liu & Bai, 2005). An important aspect of the blend properties is the miscibility of its components. Miscibility in polymer blends is assigned to specific interactions between polymeric components, which usually give rise to a negative free energy of mixing in spite of the high molecular weight of polymers. The most common interactions in the blends are hydrogen bonding, ionic and dipole, π-electrons and charge-transfer complexes. Most polymer blends are immiscible with each other due to the absence of specific interactions. Due to the similar chemical nature of chitosan and cellulose, with β-glycosidic linkages, formation of homogeneous biocomposite films can be considered (Urreaga & Orden, 2006). The main difference is primary amino groups at most of the C-2 positions in chitosan, in place of the hydroxyl groups of cellulose. According to Twu, Huang, Chang, and Wang (2003), it was expected that cellulose will be miscible with chitosan and the introduction of the amino group into cellulose will result interesting applications.

In the last years, some studies have been carried out on chitosan cellulose blends. Twu et al. (2003) used the N-methylmorpholine-N-oxide as solvent for direct dissolution of cellulose and mentioned that it would be the most promising solvent for both polysaccharides. Wu et al. (2004) prepared blends of chitosan and cellulose by casting films from trifluoroacetic. It has been shown that chitosan can modify properties of cellulose when water interaction or mechanical properties are considered. Moreover, chitosan-based matrix is limited by its water sensitivity and its poor tensile strength after wetting in water. Blending cellulose with chitosan is also expected to be a useful method to improve the mechanical properties of chitosan (Wu et al., 2004).

In the present work, we attempt to use NaOH/thiourea aqueous solutions as a common solvent to elaborate chitosan/cellulose films. The biopolymers were analyzed before and after the dissolution in the alkaline solvent to study the impact of the solvent on cellulose and chitosan. The characterization of biocomposites by infrared spectroscopy (FTIR), scanning electron microscopy (SEM), X-ray diffraction, thermal analysis and by the study of biopackaging–water interaction was performed.

2. Materials and methods

2.1. Materials

Sisal cellulose was kindly supplied by Lwarcel (Lençóis Paulista, SP, Brazil). Chitosan 244 was provided by France Chitine (Marseille, France).

2.2. Methods

2.2.1. Characterization of the biopolymers

2.2.1.1. Characterization of sisal cellulose. The degree of polymerization (DPv) of sisal was determined (25 °C) from the intrinsic viscosity of cellulose solution in CUEN (copper:ethylene diamine, 1:1, v/v) according to Tappi T 230 om-89 (1990) by employing an Ostwald shear-dilution Cannon Fenske viscosimeter (Shop Lab, São Paulo, Brazil) coupled to a thermostatic bath and circulator (Masterline Forma Scientific, Marietta, OH). The Crystallinity index (I_c) was determined by X-ray diffraction, using a VEB CARL ZEISSW-JENA URD-6 Universal Diffractometer operating at 40 kV/20 mA and λ (Cu Kα) = 1.5406 Å. I_c is calculated according the equation $I_c = 1 - I_1/I_2$, where I_1 is a minimum intensity and I_2 is a maximum intensity (Buschle-Diller & Zeronian, 1992).

2.2.1.2. Characterization of chitosan. The degree of acetylation (DA) of chitosan was determined by proton NMR. Spectra were recorded with a Brucker AC-200 spectrometer running at 200 MHz and 80 °C. Before analysis, 10 mg of chitosan was dissolved in D_2O/HCl conc. (100/1 v/v) and stirred during 24 h, at room temperature. The DA value was calculated by means of the ratio between the area corresponding to the proton resonance of the acetamide methyl groups (A_{CH_3}, δ = 2.00 ppm) and the corresponding resonance for the proton linked to C-2 of glycosamine ring (A_{H_2}, δ = 3.12 ppm): $\%DA = (A_{CH_3}/3A_{H_2}) \times 100$.

The degree of polymerization of chitosan was evaluated by the determination of the intrinsic viscosity [η] (milliliters per gram) as well as the Huggins constants, calculated in the common way from a plot η_{sp}/c versus concentration "c" of chitosan solutions. The capillary viscosimetry was carried out in an Ubbelohde-type viscometer at 25 °C on the concentration series.

The average molar mass was determined by size exclusion chromatography (SEC) using a Shimadzu SCL-10A system controller connected to a LC-10AD pump, CTO 10 column oven and equipped with RID-6A refractive index detector. The column system consisted of a preceded column SHODEX Ohpak SB-G+ and two columns SHODEX Ohpak SB (805HQ + 803HQ) with buffer solution of acetic acid and sodium acetate as the mobile phase, flowing at 0.8 mL per min at 35 °C. Before being injected into the SEC system, the chitosan buffer solution was filtered through a 0.45 μm PTFE membrane filter. Samples of Pullulan were used as standard.

2.2.2. Elaboration of films

2.2.2.1. Elaboration of homogeneous cellulose films. Films were elaborated according to a modified method of Cai et al. (2004). Cellulose was used after a mercerization process. Sheets of the sisal cellulose were crushed on an automatic system (120–18 000 rpm). Aqueous solution containing NaOH/thiourea/H_2O with 5/6/89 by weight ratio was used as the solvent of cellulose. The desired amount of cellulose (3 g) was added into 97 g of solvent at ambient temperature under a vigorous stirring. Cellulose was dissolved within 5 min under a stirring at 3000 rpm. The resulting aqueous solution was stored at −12 °C for 18 h. Solution was subjected to centrifugation at 8000 rpm for 20 min at 10 °C in order to exclude the slightly remaining undissolved part and to carry out the degasification. The resulting transparent solution was immediately cast on a polypropylene plate at a thickness of about 100 μm. The films were air-dried at room temperature for 18 h. The resulting wet films were washed with running water until pH 7 and finally dried at 20 °C and 65% relative humidity (RH) for 2 days. Materials were subsequently conditioned at 23 ± 1 °C and 50 ± 5% RH for 5 days before property measurements.

2.2.2.2. Elaboration of homogeneous chitosan films. Chitosan films were elaborated by adding 1.5 g chitosan in 98.5 g NaOH/thiourea solution as specified before. The solution was agitated for 5 min before following the same steps as mentioned for sisal cellulose films.

2.2.2.3. Elaboration of the biocomposite films. Solutions of chitosan and sisal cellulose were separately prepared. The cellulose and chitosan solutions were blended together in a 50/50 (w/w) ratio. Blends with cellulose/chitosan in a 25/75 (w/w) ratio were also elaborated for NMR relaxometry analyses. Transparent films were obtained by casting the film forming solution in polypropylene dishes under the same conditions used to obtain the pure biopolymer-based films. The materials were subsequently conditioned at 23 ± 1 °C and 50 ± 5% RH for 5 days before property measurements.

2.3. Film analyses

2.3.1. Thickness measurements

Material thickness was measured with a micrometer Lorentzen & Wettre SE050 (Lorentzen & Wettre, Saint-Germain-en-Laye, France), from six measurements per material.

2.3.2. Elemental analysis and atomic absorption

The films, as well as the original samples of cellulose and chitosan, were characterized by elemental (sulfur analysis, Perkin Elmer, Elemental Analysis 2400) and atomic absorption (sodium analysis, Hitachi, Z-8100) analyses, aiming to verify a possible presence of residual solvent system (thiourea/NaOH).

2.3.3. Morphological surface analysis by scanning electron microscopy (SEM)

SEM images of films were performed using a LEO 440 ZEISS/LEICA model operating at 15 kV. The apparatus used a tungsten filament electron source and scanned at room temperature. Samples were metalized with gold.

2.3.4. Fourier transform infrared spectroscopy (FTIR) analysis

ATR spectra were recorded by a ThermoNicolet AVATAR 370 FTIR coupled with a Nicolet Centaurus IR-microscope and treated by OMNIC software (Thermo-Nicolet, Coutaboeuf, France), between 400 and 4000 cm^{-1} using 50 scans with a resolution of 4 cm^{-1}.

2.3.5. Crystallinity index (I_c)

It was determined by X-ray diffraction, using the same procedure as in the characterization of the biopolymers.

2.3.6. Thermogravimetric analysis (TG)

The analyses were carried out in a Shimadzu TGA-50 WSI instrument on samples of films. Approximately 5 mg of sample was weighed and heated from room temperature to 600 °C at 20 °C min^{-1} under nitrogen flow rate of 20 mL min^{-1}. The data were processed using the TA50-WSI Shimadzu software.

2.3.7. Differential scanning calorimetry analysis (DSC)

The analyses were carried out in a Shimadzu DSC-50 WSI instrument from approximately 5 mg of material (sample on an aluminum pan) under nitrogen flow rate of 20 mL min^{-1}. Each sample was analyzed from two run experiments. The first run was carried out from room temperature to 110 °C at 20 °C min^{-1}, for 1 h, to remove volatile compounds and to eliminate the thermal history of the sample. The second run was accomplished at 20 °C min^{-1}, from room temperature to 350 °C.

2.3.8. Dynamic mechanical thermoanalysis (DMTA)

The measurements were carried out by using a thermal analyzer from TA Instruments model 2980. The experimental conditions were oscillation amplitude of 4 μm, 1 Hz frequency, preload of 0.15 N, heating rate of 3 °C min^{-1} and temperature range of 30–250 °C.

2.3.9. Liquid and vapor water interaction

For water contact angle meter determination, the contact angle between the material and a distilled water droplet was measured according to TAPPI T 458 om-94 (1994) and using a Dataphysics contact angle system-SCO equipped with a camera and a recording system. Resulting angle was calculated from 10 measurements. A water drop was deposited on the surface of different films. The θ angle in the interface water/film was measured at the nearest 1°. Three measurements on each film were performed at random positions.

For sorption isotherm measurements, film samples beforehand dried at 103 °C for 2 h were stored at 25 ± 1 °C in sealed glass jars containing saturated salt solutions to give different relative humidities: LiCl–H_2O, $MgCl_2$, K_2CO_3 and NaCl, respectively, for 12%, 33%, 43%, 75% RH. Aluminum dishes were weighted to the nearest 0.0001 g and about of 0.20 g of film were deposited to each dish. The water content of moisture equilibrate samples were determined after another drying at 103 °C for 2 h.

For relaxometry NMR analysis, the measurements were performed using the method presented by Bordenave, Grelier, and Coma (2007). Briefly, the NMR measurements were carried out on a Bruker Minispec PC120 spectrometer (Bruker Optics, Champ-sur-Marne, France) operating at 20 MHz proton resonance frequency corresponding to a magnetic field of 0.47 T. The $\pi/2$ pulse length is 2.8 μs and the typical value of dead time is 7 μs. The temperature of the magnet was 40 °C and the probe temperature was initially regulated at 25 °C. Before each measurement, 30 min were necessary for temperature equilibration of the samples. The Carr, Purcell, Meiboom and Gill (CPMG) sequence of measurements was used.

The CPMG sequence permits the characterization of the protons of the material by spin–spin relaxation times T_2. Spectra were acquired setting 600 echoes, with an accumulation of 1000 scans spaced out by a recycle delay of 3 s. Echo spacing of 30 ms is needed to discriminate the longest T_2 values attributed to the liquid part of the material. Usually, with the CPMG sequence, the echo amplitude detected at the time is given by $M(t) = \sum_i k_i \exp^{-t/T_{2i}}$ where T_{2i} and k_i are, respectively, the spin–spin relaxation time and the weight of the ith component of the decay. Errors in reported T_{2i} are within 2% in nominal values. Multiexponential profiles obtained by this sequence were also fitted to a sum of exponential components and had to be decomposed into their different contributions. In this study, a continuous approach has been used for the decomposition of the magnetization decay, with CONTIN, a Promencher's program. The result of the calculation is a relaxation spectrum giving intensity versus relaxation time. To study the moisture susceptibility of materials, the NMR study was conducted on samples conditioned beforehand in air-tight containers containing salt-saturated solutions at 25 °C to reach constant relative humidity: $Mg(NO_3)_2$–$6H_2O$ (53%RH) and KCl (85% RH).

2.3.10. Analysis of results

All experiments were replicated at least three times. Results were statistically analyzed using Student's *t*-test at 95% probability.

3. Results and discussion

3.1. Characterization of the biopolymers and impact of the solvent

There has been considerable research interest to prepare cellulose film for food preservation, but pure cellulose membranes were largely limited without chemical modification of the biopolymer. In addition, pure chitosan membranes were also limited due to poor mechanical strength and chemical stability of the aminopoly-

saccharide. Blending cellulose with chitosan could be an effective way to overcome the shortcomings of both biopolymers, because blending may form additional chemical bonds due to chemical interaction. The use of thiourea/NaOH as co-solvent for both macromolecules may be responsive of chemical modifications such as rupture of glycoside bonds. Some studies reported that urea seems to affect only polymer–polymer interactions (Cho, Heuzey, Begin, & Carreau, 2006). Tsaih and Chen (1997) showed that the intrinsic viscosity of chitosan increased in solution when 4 M urea was added and that this increase was more pronounced for higher molecular weight chitosan because urea breaks the intra-molecular hydrogen bonds, leads to chitosan in an extended form, and therefore have a higher intrinsic viscosity (Tsaih & Chen, 1997). Chitosan-based films are generally obtained after solubilization of chitosan in acid aqueous solutions. As specified by Cho et al. (2006), since the copolymer becomes positively charged due to the protonation of free amine groups below their pK_a (6.2), polymer–polymer interactions via hydrophobic effect and/or hydrogen bonding junctions can be hindered due to electrostatic repulsion. Urea is generally known as a hydrogen bonding disrupting agent but it can also affect hydrophobic interactions. As a result, Phillipova et al. (2001) showed reduced formation of hydrophobic domains in chitosan solutions in the presence of urea at a concentration of 7 M. As previously mentioned, thiourea was used in place of urea in this study, to allow an easier dissolution of polysaccharides. The impact of the solvent on the biopolymer structure was thus investigated by spectroscopy analyses. FTIR spectra of chitosan before and after dissolution in NaOH/thiourea displayed characteristic absorptions. The main wavenumber absorption peaks are reported in Table 1. Chitosan before dissolution showed characteristic absorption bands at 3420, 2929 and 2888 cm^{-1}, which mainly represent the —OH, —CH_2 and —CH_3 aliphatic groups, respectively. As specified by Yin, Luo, Chen, and Khutoryanskiy (2006), absorption bands at 3452, 3363 and 3313 cm^{-1} of pure chitosan films could be assigned to the OH-stretching, which overlaps with NH-stretching in the same region. Sionkowska, Wisniewski, Skopinska, Kennedy, and Wess (2004) mentioned that the amino group has a characteristic absorption band in the region of 3400–3500 cm^{-1}, which is masked by the broad absorption band from the —OH group. The peaks at 2929 and 2888–2860 cm^{-1} were due to CH-stretching. Bands at 1660 and 1631 could be attributed to C=O-stretching (amide I) and NH-bending (amide II), respectively, and confirmed that chitosan is a partially deacetylated product. The absorption band at 1429 cm^{-1} could be due to CH- and OH-vibrations (Yin et al., 2006). Indeed, according to Sionkowska et al. (2004), a band at 1414 cm^{-1} is assigned to hydroxyl vibration of primary alcoholic group. Basic characteristics of chitosan were also showed by the band near 1166 cm^{-1}, which overlaps with the characteristic absorption band near 1140 cm^{-1}, assigned to anti-symmetric stretching of the C—O—C bridge, and 1074 and 1030 cm^{-1} which are skeletal vibrations involving the C—O-stretching (Yin et al., 2006). The strong peaks at 1030 and 1074 are characteristic peaks of a saccharide structure. The bands at 2929 and 2860 cm^{-1} (CH-stretching) depressed or became hardly detectable after alkaline solubilization compared to the spectra of the parent chitosan. Moreover, an alteration of the region both at 1660 (amide CO-stretching) and at 1380 cm^{-1} (C—CH_3 amide stretching) was noted. This could be due to a decrease in the acetylation degree after alkali treatment (Muzzarelli, Tosi, Francescangeli, & Muzzarelli, 2003).

The FTIR spectra of cellulose before and after NaOH/thiourea dissolution, also presented characteristic absorption peaks (Table 1). Peak near 3380 cm^{-1} was due to OH-stretching and peaks at 2904–2879 cm^{-1} were assigned to CH-stretching. The band at 1637 or 1644 cm^{-1}, before and after alkaline dissolution, respectively, could be due to water in the amorphous region (Yin et al., 2006). The strong band at 1055 cm^{-1} was assigned to skeletal vibrations involving the C—O-stretching. The absorption band at 893 cm^{-1} belongs to β-anomers or β-linked glucose polymers, and the absorption peak in NaOH/thiourea cellulose became more intense than the corresponding one in the original cellulose. These observations were in accordance with results obtained by Zhang et al. (2002), with a lower difference due to the use of mercerized cellulose. This is characteristic of transition from cellulose I to II. Following this first molecular study, it seemed that the solvent did not lead to a decomposition or derivatization of the polymers. According to Zhang et al. (2002), the ^{13}C NMR results suggested the absence of derivatization of cellulose after solubilization of the biopolymer in alkaline solvent.

The impact of the solvent on the biopolymer was then investigated by the determination of the average molar mass of chitosan (Rinaudo, Milas, & Ledung, 1993) and cellulose before and after dissolution in NaOH/thiourea. The results are presented in Table 2. According to Jayaraju, Raviprakash, Keshavayya, and Rai (2006), chitosan exhibits polyelectrolyte properties in solution, because of the presence of free amino groups in its backbone. In the absence of salt, there is an abnormal increase in the viscosity of the more dilute solution, because of an enlarged effective volume due to charge repulsion, and thereby it stretches out of the mole-

Table 1
Infrared absorption bands of chitosan and sisal cellulose before and after dissolution in NaOH/thiourea.

	Before dissolution	After dissolution	Assignment
Chitosan	3420		OH- and NH-stretching
	2929	*Depressed*	CH-stretching
	2888		
	2860	*Depressed*	
	1660	*Depressed*	C=O-stretching (amide I)
	1631		NH-bending (amide II)
	1429	*Depressed*	CH- and OH-vibrations
	1381	*Depressed*	C—CH_3 amide stretching
	1166–1140	*Increased*	Anti-symmetric stretching of C—O—C bridge
	1074		Skeletal vibrations involving the C—O-stretching
	1030		
Sisal cellulose	3381		OH-stretching
	2904		CH-stretching
	2879		
	1637	2138 Shift 1644 *Increased*	Water in the amorphous region
	1055		Skeletal vibrations involving the C—O-stretching
	1370		CH- and OH-vibrations
	1159	Shift 1169	Anti-symmetric stretching of C—O—C bridge
	1055	*Depressed*	Skeletal vibrations involving the C—O-stretching
	893	Shift 897 *Increased*	

Table 2
Viscometric average molar mass of the studied sisal cellulose and chitosan.

	Average molar mass (g mol^{-1})	
	Before dissolution in NaOH/thiourea	After dissolution in NaOH/thiourea
Sisal cellulose	118 200	18 500
Chitosan	22 000*	6500*

* Determined considering the DA and the parameters (M–H equation, *K*, *a*, parameters) described in Rinaudo, Milas, and Ledung (1993).

cule. Due to the doubts on the DPv obtained for chitosan, the average molecular weight from viscosimetry analysis could be used in first approximation, to show an important depolymerization by the solvent. However, the molar mass of the chitosan was also obtained via SEC. The average molecular weights were $M_n \sim 41\,800$ g/mol and $M_w \sim 193\,000$ g/mol, leading to a ratio M_w/M_n about of 4.6. As a result, dissolution in NaOH/thiourea led to chain depolymerization of both, sisal cellulose and chitosan, mainly due to the reaction with hydroxyl anions. This is a very important remark, because, to the best of our knowledge, there is no information about this fact in the literature. It seems that at least in part, the easiness for the dissolution of chitosan and cellulose in NaOH/thiourea comes from their considerable decrease in average molar mass in this solvent system. This can be a problem for some application of these polysaccharides after dissolution in this solvent system, but for the preparation of films, it can facilitate the process. The average degree of acetylation of the original chitosan (30%) shifted to 26% for the sample recovered after dissolution.

According to these results, the dissolution of chitosan in thiourea/NaOH, at least under the conditions of the present study, cannot be considered exactly as a "true" dissolution process, because the average molecular weight is lower and the structure of the polysaccharide is different, relating to the original sample.

3.2. Film analyses

3.2.1. Residual solvent system

In order to verify a possible presence of residual solvent system into the films, the content of sulfur (thiourea) and sodium (NaOH) were evaluated by elemental analysis and atomic absorption, respectively (Table 3). The data in Table 3 show that there was no residual thiourea into the films (S% = 0.00). Concerning the sodium content, the original samples of sisal cellulose and chitosan have the same percentage found for the biocomposite film, *i.e.* the dissolution process did not introduce this element.

3.2.2. Morphology

SEM views of cellulose, chitosan as well as biocomposite films are shown in Fig. 1. Luo et al. (2008) specified that SEM data serve as good evidence for complete miscibility between chitosan and hydroxy ethyl cellulose in the solid state, due to fully homogeneous structure obtained with no sign of phase separation. The morphology of the cellulose matrix showed fibrous structure, whereas homogeneous chitosan films displayed a relatively smooth morphology with a nonfibrous structure. The biocomposites led to an intermediate organization. The chitosan matrix recovered the cellulose network implying good adhesion between the polymer matrices. Moreover, as already obtained by Lu et al. (2006) on starch–cellulose biocomposite and by Luo et al. (2008) on chitosan–hydroxy ethyl cellulose blends, no large agglomerates were observed. This was probably due to the hydrogen bonding interactions between the hydroxyl groups of the components.

Table 3
Contents of sulfur and sodium in films.

	Chitosan	Sisal cellulose	Chitosan/sisal cellulose biocomposite
% S	0.00	0.00	0.00
% Na	0.21 ± 0.02	0.35 ± 0.05	0.55 ± 0.01

3.2.3. Crystallinity

The crystallinity of the cellulose, chitosan or biocomposite films is presented in Table 4. The results indicated that the crystallinity of sisal cellulose and its film were the same. Zhang et al. (2005) showed that the transition from cellulose I to II had taken place after solubilization of cellulose in aqueous NaOH/urea. These authors obtained a value of the crystallinity index of the corresponding films range from 48% to 56%, which are lower than that of their original cellulose (73%). In the present work, the decrease in crystallinity caused by the dissolution in NaOH/thiourea could be counterbalanced by two factors, which increase the concentration of crystallites (i) the cellulose was degraded by NaOH/thiourea, which probably affected mainly the noncrystalline domain, and (ii) residual hemicelluloses, present in noncrystalline domain, could be dissolved in this solvent system.

For the chitosan film, I_c values of the films were considerably lower than that of chitosan before dissolution. These results are in accordance with the study of Zhang et al. (2005) conducted on cellulose, and can be taken as an indication that the interactions of chitosan with the solvent system were higher, when compared with sisal. As reported by Cho et al. (2006), two mechanisms are proposed about the effect of urea on hydrogen bonding interactions, one is that urea only has an impact on the intermolecular interaction, while the other is that urea breaks intra-molecular hydrogen bound, and causes a change in molecular conformation. This latter leads either to a breakdown of the hydrogen-bonded structure of the solvent or to a structuring breaking effect. Urea could also influence hydrophobic interactions in chitosan (Phillippova et al., 2001). Finally, when the biocomposites were analyzed, higher I_c than chitosan films was obtained probably due to the sisal component. The addition of cellulose to chitosan makes the material less amorphous (I_c from 36% to 53% for chitosan and biocomposite films, respectively). It is interesting to note that, unlike the chitosan blends with hydroxy ethyl cellulose reported previously

Table 4
Crystallinity index (I_c) of sisal cellulose, chitosan, their related films and biocomposite film.

Sample	I_c (%)
Sisal before dissolution in NaOH/thiourea	54
Sisal film	54
Chitosan before dissolution in NaOH/thiourea	64
Chitosan film	36
Sisal cellulose/chitosan biocomposite film	53

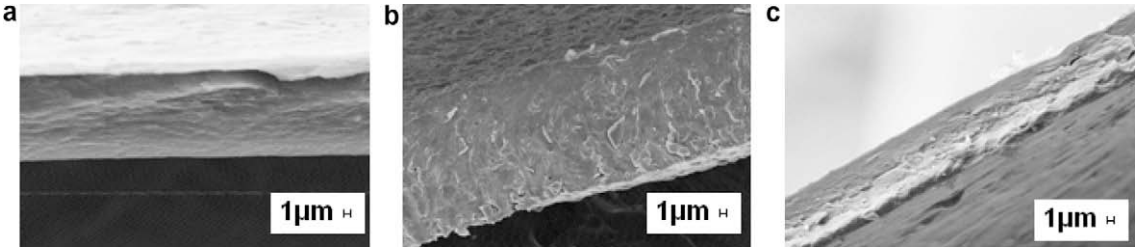

Fig. 1. SEM images (transversal views) of films based on (a) chitosan, (b) sisal, (c) sisal cellulose/chitosan biocomposite.

(Luo et al., 2008) the crystalline structure of cellulose were unchanged, and it seems that the chitosan addition does not restrict the ability of macromolecules to form ordered region typical for crystalline domains. Moreover, this could suggest a cooperative effect of both macromolecules to the crystalline domains

3.2.4. Thermal analyses

The DSC analysis showed that in the first scanning all the samples presented an endothermic peak near 100 °C due to the elimination of residual humidity. This peak was not observed in the second scanning (Fig. 2a).

The chitosan film presented an endothermic peak near 225 °C, and an exothermic peaks near 275 °C, which can be also observed on TGA curves (Fig. 2b). Theses peaks could be due to the chain deacetylation and to decompositions involving the main chain (Ou et al., 2008). A thermal decomposition step followed by volatilization of by products could be detected both as endothermic or exothermic peaks, depending on the balance between both processes. Apparently, in the present work, in the first peak observed, the endothermic process masked the exothermic one. This could be due to the decomposition of acetylated units, already correlated to an endothermic process (Nieto & Peniche-Covas, 1991). In the literature various remarks were made on the thermal decomposition of chitosan, since only exothermic (Ou et al., 2008) or only endothermic (Chuang, Young, Yao, & Chiu, 1999) peaks were mentioned. The thermal properties of chitosan are dependant on degree of acetylation, crystallinity, average molecular weight and probably are at the origin of the different data found in the literature.

Thermal degradation of cellulose, which occurs between 250 and 350 °C, leads to depolymerization and to the formation of 1,6-anhydroglucose. The thermolysis reaction of cellulose (and hemicelluloses, when these polysaccharides are present) occur by the cleavage of glycoside bonds, C—H, C—O, C—C bonds, as well as by dehydration, decarboxylation and decarbonylation. Considering the mixture arising from the degradation of cellulose, levoglucosan, produced by transglycosylation intra-molecular reactions (Scheirs, Camino, & Tumiatti, 2001) is the most abundant product (Meier & Faix, 1999). The DSC curve related to the biocomposite show that the endothermic peak near 225 °C for chitosan film disappeared, and two exothermic peaks can be observed near 285 (low intensity) and 315 °C (high intensity). This can be taken as an indication that the interactions between chitosan and cellulose influenced their thermal decomposition, and probably the peak at high temperature comprised the decomposition of both polysaccharides.

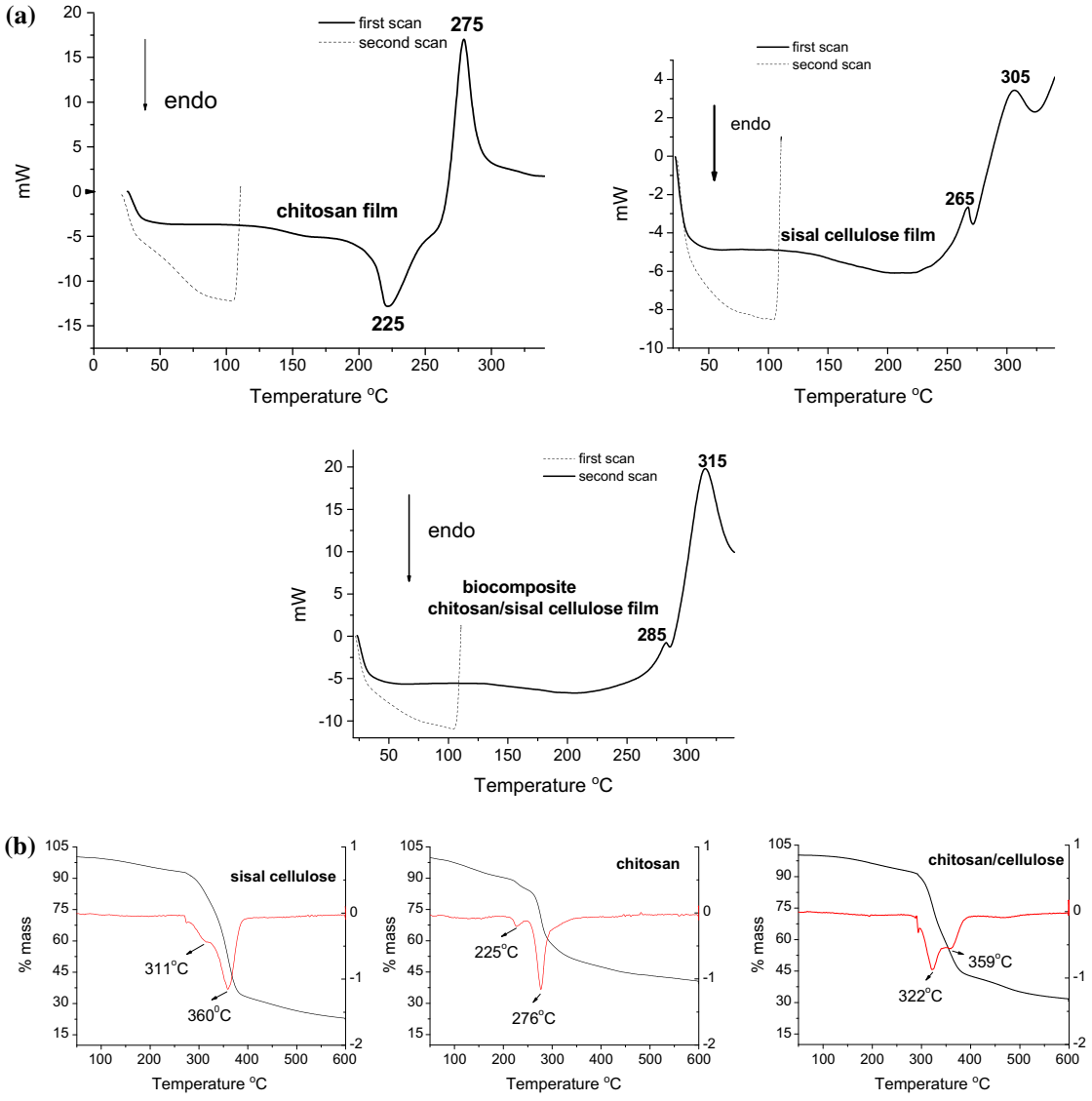

Fig. 2. DSC (a) and TG (b) curves of films based on chitosan, sisal and chitosan/cellulose biocomposite.

The TGA results indicated that the maximum weight loss was higher and occur at lower temperature for chitosan film, compared to sisal film. The maximum weight loss of biocomposite was similar to that of chitosan and occurs at a temperature between those of chitosan and sisal films (Table 5). As also observed by Luo et al. (2008), on chitosan/cellulose ether blends, the thermal stability of the blend is intermediate between the stability of the pure polymers.

Water volatilization can occur in a wide temperature interval, due to the strong hydrogen bonds developed between water and chitosan/cellulose polar groups. Thus, the TGA results with respect to the maximum weight loss indicated that the water absorption was higher for chitosan and biocomposite film, when compared to sisal, in agreement with the previous results. In addition, the TGA results could also indicate that a high amount of volatiles was produced during the thermal decomposition of chitosan, maybe due to the presence of acetylated units in this polysaccharide.

Fig. 3 shows that the curves of storage modulus as a function of temperature have different profile for chitosan, sisal cellulose and biocomposite films. The storage modulus increased during the scanning for both chitosan and biocomposite films, whereas continuous decrease was observed for sisal film. As previously mentioned, chitosan and chitosan/cellulose biocomposite are more hygroscopic than sisal cellulose. The volatilization of the retained water eliminated its plasticizer effect, increasing then the storage modulus of those films during the scanning. Considering that above near 175 °C none of the three films contain residual water, it can be seen that both, chitosan and biocomposite films were stiffer than the cellulose one.

3.2.5. Liquid and water vapor interaction

An interesting result is that chitosan film elaborated with NaOH/thiourea led to only 11% (w/w) of solubilization in water and that the material maintained its integrity (data not shown). Indeed, the solvent most frequently used, *i.e.* acetic acid, led to chitosan films completely soluble in water, as previously observed (Möller et al., 2004). The low solubility in water of chitosan films obtained by coagulation from NaOH/thiourea will be interesting for food preservation applications.

3.2.5.1. Contact angle. The contact angle for the chitosan film was close to 95° (Fig. 4). However, it was observed a deformation in the surface of the chitosan film when the contact between water drop and film surface occurred, as a consequence of the projection of the film surface toward the drop of water, due to the high affinity between the surface and water. This deformation affected the contact angle and it was not therefore possible to use the obtained value as strictly indicative of the hydrophilic/hydrophobic character of this film, since the surface was no longer flat at the time of contact with water. A similar behavior was observed for the biocomposite. It must be pointed out that similar results, *i.e.* high contact angles for chitosan films, can be found in the literature (Chen, Wang, Mao, Liao, & Hsieh, 2008; Chen, Wang, Mao, & Yang, 2007; Tsai & Wang, 2008), although the high angle was attributed, for example, to the hydrophobic backbone of chitosan chains (Chen et al., 2008; Tsai & Wang, 2008). By contrast, the contact angle of sisal cellulose film is near 50°, and no deformation was observed in its surface as a consequence of the contact with the drop of water.

3.2.5.2. Sorption isotherms. No significant difference was obtained between chitosan and sisal cellulose films. However, Fig. 5 shows that for high relative humidity sisal film was less hygroscopic that chitosan film and that the biocomposite film had an intermediate behavior.

3.2.5.3. NMR relaxometry. In order to refine the study of the water–material interaction and to obtain more information about the behavior of the different films, studies based on the NMR relaxometry were carried out (Bordenave, 2008). T_2 parameter gives information on proton mobility and could be used to identify the various states of water in the material. This technique allows to evaluate the relative amount of water in the material and thus, qualitatively, the various forms of water in the material. Materials were previously stored at two relative humidities (RH) before NMR analysis (53% or 85%). Results are presented in Table 6. When RH is higher, the behavior of the chitosan film elaborated from the NaOH/thiourea solutions showed a slight increase in the surface of the second peak close to 0.2 or 0.5 ms. This is a very different behavior compared to the conventional acetic acid chitosan film (Bordenave et al., 2007), which showed a very strong peak increase at high RH. It seems that the chitosan solubilized in sodium

Table 5
Films TGA data, temperature of maximum decomposition (T_d) and respective percentage of material weight loss.

Film	T_d (°C)	Weight loss (%)
Chitosan	278	74
Sisal	360	50
Sisal cellulose/chitosan biocomposite	323	74

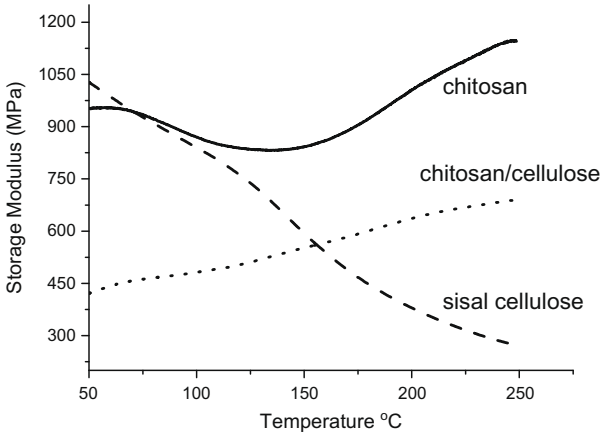

Fig. 3. Storage modulus as a function of temperature for films based on chitosan, sisal and chitosan/sisal cellulose biocomposite.

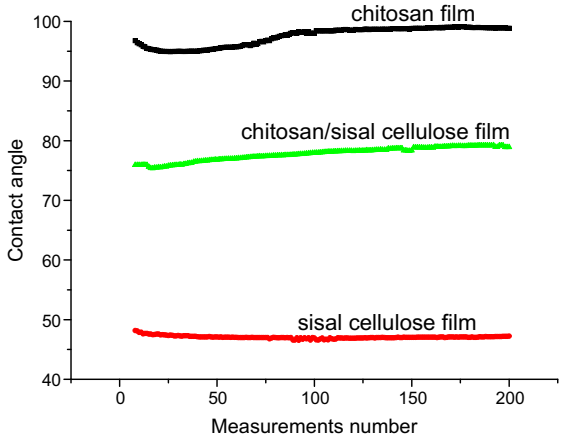

Fig. 4. Water contact angle for films based on chitosan, sisal cellulose or chitosan/sisal cellulose biocomposite.

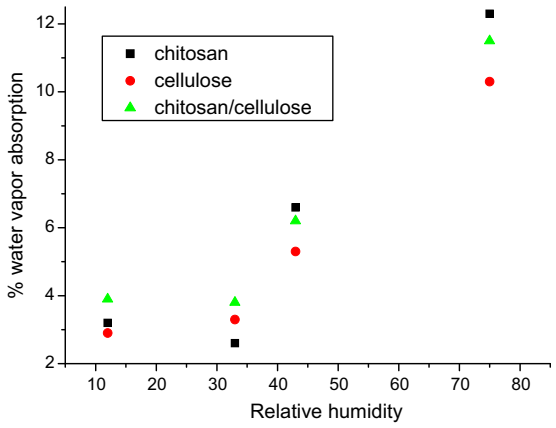

Fig. 5. Sorption isotherm for films based on chitosan, sisal cellulose and chitosan/sisal cellulose biocomposite.

hydroxide was less sensitive to water vapor and led to less free water. This could be notably attributed to the lower acetylation degree after alkaline solubilization. Increase in the storage RH did not lead to the formation of a hydrogel, contrary to film from acetic acid chitosan (Bordenave et al., 2007). This could be due to the lower average molecular weight after alkaline treatment.

The comparison between sisal cellulose and chitosan films beforehand conditioned at 53% or 85% RH, showed three main peaks for cellulose and only two for chitosan (Table 6). As expected, the proton mobility in cellulose film increased as RH increased, suggesting "layers with increasingly free water". At 50% RH, peak at 0.2 ms observed for the chitosan film (area 32.4%), seemed to move close to 0.6 ms for the cellulose (area 36.2%), suggesting higher ratio free/bound water molecules for cellulose film. The same phenomenon was observed at 85% RH. As a result, chitosan and cellulose films exhibited different behavior with respect to the water vapor. Chitosan seemed to be more sensitive to moisture variations and there was more bound water in chitosan film than in cellulose one.

The behavior of chitosan or cellulose with respect to water could be due, as mentioned by Wu et al. (2004), to a stronger affinity of chitosan to water and to the larger volume of amino side groups (19 $cm^3\ mol^{-1}$) on chitosan compared to the hydroxyl side groups (13 $cm^3\ mol^{-1}$) on cellulose. In addition, the higher basicity of nitrogen atom (from chitosan amino group) when compared to oxygen atom (from cellulose —OH groups) leads to more intense hydrogen bonds with water molecules, which can also contribute to the observed NMR results.

The comparison of biocomposite with homogeneous films of chitosan and sisal cellulose showed that the behavior of the biocomposite was the same than that of the chitosan one (Table 6). This result showed that the water–chitosan interactions were dominant and that the aminopolysaccharide fraction imposed its behavior. To confirm this hypothesis, an increase of the chitosan fraction in the biocomposite was then studied by low resolution NMR. A very weak increase in the second peak area was observed due to a more hydrophilic structure but it did not practically influence the behavior of the material with respect to water vapor and biopolymer miscibility. This result confirmed that the chitosan

Table 6
T_2 (ms) of the different materials after storage at 53% or 85% of relative humidity and comparison of chitosan, cellulose and sisal cellulose/chitosan biocomposite films with two different ratio of biopolymers.

	53% Relative humidity			
Chitosan				
Peak time interval (ms)	(0.007–0.056)	(0.183–0.292)	(1.920–2.420)	
Relaxation time at the maximum of the peak (ms)	0.028	0.231	1.92	
Peak area (relative unit, %)	67.4	32.4	0.2	
Sisal cellulose				
Peak time interval (ms)	(0.007–0.056)	(0.114–0.183)	(0.468–0.748)	(9.930–15.90)
Relaxation time at the maximum of the peak (ms)	0.028	0.144	0.592	12.6
Peak area (relative unit, %)	61.01	2.5	36.2	0.2
Cellulose/chitosan biocomposite (50/50)				
Peak time interval (ms)	(0.007–0.045)	(0.183–0.292)	(6.210–9.930)	
Relaxation time at the maximum of the peak (ms)	0.022	0.231	7.85	
Peak area (relative unit, %)	70.9	28.9	0.2	
Cellulose/chitosan biocomposite (25/75)				
Peak time interval (ms)	(0.007–0.056)	(0.231–0.370)	(3.880–6.210)	
Relaxation time at the maximum of the peak (ms)	0.028	0.292	4.91	
Peak area (relative unit, %)	65.9	33.9	0.2	
	85% Relative humidity			
Chitosan				
Peak time interval (ms)	(0.007–0.045)	(0.370–0.592)		
Relaxation time at the maximum of the peak (ms)	0.022	0.468		
Peak area (relative unit, %)	61.3	39.7		
Sisal cellulose				
Peak time interval (ms)	(0.007–0.090)	(0.183–0.370)	(0.592–1.200)	(32.20–51.50)
Relaxation time at the maximum of the peak (ms)	0.035	0.292	0.947	40.7
Peak area (relative unit, %)	41.5	10.3	47.7	0.5
Cellulose/chitosan biocomposite (50/50)				
Peak time interval (ms)	(0.007–0.056)	(0.370–0.592)		
Relaxation time at the maximum of the peak (ms)	0.028	0.468		
Peak area (relative unit, %)	56.9	43.1		
Cellulose/chitosan biocomposite (25/75)				
Peak time interval (ms)	(0.007–0.056)	(0.370–0.592)		
Relaxation time at the maximum of the peak (ms)	0.028	0.468		
Peak area (relative unit, %)	50	50		

fraction imposed its behavior to the biocomposite, from 50% of aminopolysaccharide in the blend.

According to Wu et al. (2004), the chitosan/cellulose blends using trifluoroacetic acid as co-solvent showed mechanical and dynamic mechanical thermal properties almost dominated by cellulose, also suggesting the non-miscibility of both biopolymers. These authors specified that intermolecular hydrogen bonds of cellulose were break down to form cellulose-chitosan hydrogen bonds; however, the intra-molecular and intra-strand hydrogen bonds hold the network flat. Cellulose maintained its mechanical properties in the blend due to the remaining of its intra-molecular and intra-strand hydrogen bound. In our case, the non-miscibility of both biopolymers in alkaline solvent could lead to water interactions considerably dominated by chitosan, which coated the cellulose matrix. It will be interesting, in the future, to study dynamic mechanical of such blends. Hasegawa et al. (Hasegawa, Isogai, Onabe, Usuda, & Atalla, 1992; Hasegawa et al., 1994, 1994) studied interactions between cellulose and chitosan molecules in cellulose–chitosan blend films, also prepared using trifluoroacetic acid as co-solvent for both polysaccharides. Cellulose crystallinity in the blend films decreased as chitosan content increased and mechanical properties reached a maximum around 30% chitosan content in the blend. These authors suggested the presence of interactions between cellulose, chitosan, and water molecules in the films. However, Raman analyses (Hasegawa, Isogai, Onabe, Usuda, & Atalla, 1992) showed that cellulose and chitosan molecules in the blend films seemed to have the same secondary structures as those in 100% cellulose and 100% chitosan films, respectively. Thus, these results indicated the presence of interactions in the interfacial region between small domains of cellulose and chitosan. The presence of chitosan molecules may lead to decrease in the domain size of cellulose, and to increase in the interfacial region between cellulose and chitosan domains.

4. Conclusion

In this study, improvement of sisal cellulose film properties was investigated by chitosan association. Biocomposite films were then successfully prepared using NaOH/thiourea as solvent. The NaOH/thiourea led to chain depolymerization of both biopolymers, and to some deacetylation of chitosan, without a dramatic loss of film forming capacities. The contact angle analyses pointed out important aspects, normally not considered when contact angles of materials based on chitosan are discussed in the literature, *i.e.*, the deformation that can occur at the surface due to the high affinity of these materials with the drop of water.

It was shown that the crystalline character of the biocomposite was close to that of cellulose film and that interactions with water vapor were dominated by the chitosan fraction. We have demonstrated that blending cellulose with chitosan results in the formation of films with a less brittle structure.

References

Arvanitoyannis, I., Kolokuris, I., Nakayama, A., Yamamoto, N., & Aiba, S. (1997). Physicochemical studies of chitosan–poly(vinyl alcohol) blends plasticized with sorbitol and sucrose. *Carbohydrate Polymers, 34*, 9–19.

Arvanitoyannis, I. S., Nakayama, A., & Aiba, S. L. (1998). Chitosan and gelatin based edible films: State diagrams, mechanical and permeation properties. *Carbohydrate Polymers, 37*, 371–382.

Bordenave, N. (2008). Conception, étude et réduction de l'hydrophilie d'emballage antimicrobiens à base de papier et de chitosane. Thesis, Université Bordeaux 1.

Bordenave, N., Grelier, S., & Coma, V. (2007). Water and moisture susceptibility of chitosan and paper-based materials: structure–properties relationships. *Journal of Agricultural and Food Chemistry, 55*, 9479–9488.

Buschle-Diller, G., & Zeronian, S. H. (1992). Enhancing the reactivity and strength of cotton fibers. *Journal of Applied Polymer Science, 45*, 967–979.

Cai, J., Zhang, L., Zhou, J., Li, H., Chen, H., & Jin, H. (2004). Novel fibers prepared from cellulose in NaOH/urea aqueous solution. *Macromolecular Rapid Communications, 25*, 1558.

Cao, Y., Wu, J., Li, H. Q., Zhang, Y., Zhang, J., & He, J. S. (2009). Room temperature ionic liquids (RTILs): A new and versatile platform for cellulose processing and derivatization. *Chemical Engineering Journal, 147*, 13–21.

Chen, C. H., Wang, F. Y., Mao, C. F., Liao, W. T., & Hsieh, C. D. (2008). Studies of chitosan: II. Preparation and characterization of chitosan/poly (vinyl alcohol)/gelatin ternary blend films. *International Journal of Biological Macromolecules, 43*, 37–42.

Chen, C. H., Wang, F. Y., Mao, C. H., & Yang, C. H. (2007). Studies of chitosan: I. Preparation and characterization of chitosan/poly(vinyl alcohol) blend films. *Journal of Applied Polymer Science, 105*, 1086–1092.

Cho, J., Heuzey, M. C., Begin, A., & Carreau, P. J. (2006). Effect of urea on solution behavior and heat-induced gelation of chitosan-β-glycerophosphate. *Carbohydrate Polymers, 63*, 507–518.

Chuang, W. Y., Young, T. H., Yao, C. H., & Chiu, W. Y. (1999). Properties of the poly(vinyl alcohol)/chitosan blend and its effect on the culture of fibroblast in vitro. *Biomaterials, 20*, 1479–1487.

Coma, V. (2008). A review: Bioactive packaging technologies for extended shelf life of meat-based products. *Meat Sciences, 78*, 90–103.

Coma, V., Martial-Gros, A., Garreau, S., Copinet, A., Salin, F., & Deschamps, A. (2002). Edible anti-microbial films based on chitosan matrix. *Journal of Food Sciences, 67*, 1162–1169.

Desbrières, J. (2002). Viscosity of semiflexible chitosan solution: Influence of concentration, temperature, and role of intermolecular interactions. *Biomacromolecules, 3342*, 3349.

Feng, L., & Che, Z. I. (2008). Research progress on dissolution and functional modification of cellulose in ionic liquids. *Journal of Molecular Liquids, 142*, 1–5.

Fimbeau, S., Grelier, S., Copinet, A., & Coma, V. (2005). Novel biodegradable films made from chitosan and poly(lactic acid) with antifungal properties against mycotoxinogen strains. *Carbohydrate Polymers, 65*, 185–193.

Hasegawa, M., Isogai, A., Kuga, S., & Onabe, F. (1994). Preparation of cellulose–chitosan blend film using chloral/dimethylformamide. *Polymer, 35*, 983–987.

Hasegawa, M., Isogai, A., Onabe, F., & Usuda, M. (1992). Dissolving states of cellulose and chitosan in trifluoroacetic acid. *Journal of Applied Polymer Science, 45*, 1857–1863.

Hasegawa, M., Isogai, A., Onabe, F., Usuda, M., & Atalla, R. H. (1992). Characterization of cellulose–chitosan blend films. *Journal of Applied Polymer Science, 45*, 1873–1879.

Isogai, A., & Atalla, R. H. (1992). Preparation of cellulose–chitosan polymer blends. *Carbohydrate Polymers, 19*, 25–28.

Jayaraju, J., Raviprakash, S. D., Keshavayya, J., & Rai, S. K. (2006). Miscibility studies on chitosan/hydroxpropylmethylcellulose blend in solution by viscosity, ultrasonic velocity, density and refractive index methods. *Journal of Applied Polymer Science, 102*, 2738–2742.

Kumar, G., Bristow, J. F., Smith, P. J., & Payne, G. F. (2000). Enzymatic gelation of the natural polymer chitosan. *Polymer, 41*, 2157–2168.

Li, Z., Zhuang, X., Liu, X., Guan, Y., & Yao, K. (2002). Study on antibacterial O-carboxymethylated chitosan/cellulose blend film from LiCl/*N*,*N*-dimethylacetamide solution. *Polymer, 43*, 1541–1547.

Liu, C., & Bai, R. (2005). Preparation of chitosan/cellulose acetate blend hollow fibers for adsorptive performance. *Journal of Membrane Science, 267*, 68–77.

Lu, Y., Weng, L., & Cao, X. (2006). Morphological, thermal and mechanical properties of ramie crystallites—Reinforced plasticized starch biocomposites. *Carbohydrate Polymers, 63*, 198–204.

Luo, K., Yin, J., Khutoryanskaya, O. V., & Khutoryanskiy, V. V. (2008). Mucoadhesive and elastic films based on blends of chitosan and hydroxyethylcellulose. *Macromolecular Bioscience, 8*, 184–192.

Meier, D., & Faix, O. (1999). State of the art of applied fast pyrolysis of lignocellulosi materials—A review. *Bioresource Technology, 68*, 71–77.

Molinaro, G., Leroux, J. C., Damas, J., & Adam, A. (2002). Biocompatibility of thermosensitive chitosan-based hydrogels an in vivo experimental approach to injectable biomaterials. *Biomaterials, 23*, 2717–2722.

Möller, H., Grelier, S., Pardon, P., & Coma, V. (2004). Antimicrobial and physicochemical properties of chitosan–HPMC based films. *Journal of Agricultural and Food Chemistry, 52*, 6585–6591.

Muzzarelli, R. A. A., & Muzzarelli, C. (2005). Chitosan chemistry: Relevance to the biomedical sciences. *Advances in Polymer Science, 186*, 151–209.

Muzzarelli, C., Tosi, G., Francescangeli, O., & Muzzarelli, R. A. A. (2003). Alkaline chitosan solutions. *Carbohydrate Research, 338*, 2247–2255.

Nieto, J. M., & Peniche-Covas, C. (1991). Characterization of chitosan by pyrolysis-mass spectrometry, thermal analysis and differential scanning calorimetry. *Thermochimica Acta, 176*, 63–68.

Ou, C. Y., Li, S. D., Li, C. P., Zhang, C. H., Yang, L., & Chen, C. P. (2008). Effect of cupric ion on thermal degradation of chitosan. *Journal of Applied Polymer Science, 109*, 957–962.

Park, I. K., Kim, T. H., Park, Y. H., Shin, B. A., Choi, E. S., Chowdhury, E. H., et al. (2001). Galactosylated chitosan-graft-poly(ethylene glycol) as hepatocyte-targeting DNA carrier. *Journal of Controlled Release, 76*, 349–362.

Phillipova, O. E., Volkov, E. V., Sitnikova, N. L., Khokhlov, A., Desbrieres, J., & Rinaudo, M. (2001). Two types of hydrophobic aggregates in aqueous solution of chitosan an its hydrophobic derivatives. *Biomacromolecules, 2*, 483–490.

Ramos, L. A., Assaf, J. M., El Seoud, O. A., & Frollini, E. (2005). Influence of the supramolecular structure and physicochemical properties of cellulose on its dissolution in a lithium chloride/*N*,*N*-dimethylacetamide solvent system. *Biomacromolecules, 6*, 2638–2647.

Rinaudo, M., Milas, M., & Ledung, P. (1993). Characterization of chitosan. Influence of ionic strength and degree of acetylation on chain expansion. *International Journal of Biological Macromolecules, 15*, 281–285.

Scheirs, J., Camino, G., & Tumiatti, W. (2001). Overview of water evolution during the thermal degradation. *European Polymer Journal, 37*, 933–942.

Siddaramaiah, K. P., Divya, K. H., Mhemavathi, B. T., & Manjula, D. S. (2006). Chitosan/HPMC polymer blends for developing transdermal drug delivery systems. *Journal of Macromolecular Science—Pure and Applied Chemistry, 43*, 601–607.

Sionkowska, A., Wisniewski, M., Skopinska, J., Kennedy, C. J., & Wess, T. J. (2004). Molecular interactions in collagen and chitosan blends. *Biomaterials, 25*, 795–801.

TAPPI 458 om-94 (1994). Surface wettability of paper (angle contact method). *Tappi test methods*. Atlanta: Tappi Press.

Tappi T 230 om-89 (1990). Viscosity of pulp (capillarity viscosimeter method). *TAPPI test methods*. Atlanta: Tappi Press.

Tsai, H. S., & Wang, Y. Z. (2008). Properties of hydrophilic chitosan network membranes by introducing binary crosslink agents. *Polymer Bulletin, 60*, 103–113.

Tsaih, M. H., & Chen, R. H. (1997). Effect of molecular weight and urea on the conformation of chitosan molecules. *International Journal of Biological Macromolecules, 20*, 233–240.

Twu, Y. K., Huang, H. I., Chang, S. Y., & Wang, S. L. (2003). Preparation and sorption activity of chitosan/cellulose blend beads. *Carbohydrate Polymers, 54*, 425–430.

Urreaga, J. M., & Orden, M. U. (2006). Chemical interactions and yellowing in chitosan-treated cellulose. *European Polymer Journal, 42*, 2606–2616.

Wu, Y. B., Yu, S. H., Mia, L., Wu, C. W., Shyu, S. S., Peng, C. K., et al. (2004). Preparation and characterization on mechanical and antibacterial properties of chitosan/cellulose blends. *Carbohydrate Polymers, 57*, 435–440.

Yin, J., Luo, K., Chen, X., & Khutoryanskiy, V. V. (2006). Miscibility studies of the blends of chitosan with some cellulose ethers. *Carbohydrate Polymers, 63*, 238–244.

Zhang, L., Mao, Y., Zhou, J., & Cai, J. (2005). Effects of coagulation conditions on the properties of regenerated cellulose films prepared in NaOH/urea aqueous solution. *Industrial & Engineering Chemistry Research, 44*, 522–529.

Zhang, L., Ruan, D., & Gao, S. J. (2002). Dissolution and regeneration of cellulose in NaOH/thiourea aqueous solution. *Journal of Polymer Science, 40*, 1521–1529.

Zhao, L., Mitomo, H., & Yosh, F. (2008). Synthesis of pH-sensitive and biodegradable CM-cellulose/chitosan polyampholytic hydrogels with electron beam irradiation. *Journal of Bioactive and Compatible Polymers, 23*, 319–333.